



## **Structural and Optical properties of ZnO/PS nano composite before and after vacuum annealing treatment**

**Lakshmipriya Venugopal<sup>1\*</sup> and Prithvikumaran Natarajan<sup>1</sup>**

<sup>1</sup>Nano Science Research Lab, Department of Physics, VHNSN College, Virudhunagar, Tamilnadu, India

**Abstract :** The nanocrystalline ZnO thin film was coated on porous silicon substrate by sol-gel spin coating method. Porous silicon (PS) substrates were prepared by electrochemical anodization on p-type silicon wafers of (100) orientation for various current densities. Surface modification of PS by ZnO and its structural and optical properties before and after vacuum annealing treatment were studied. It is observed that (002) oriented ZnO thin film was formed on PS substrate. It is found that the size of ZnO grains is 49 nm and after vacuum annealing treatment the grain size of ZnO on PS increases from 49 to 61 nm. SEM images show that the pore filling of ZnO on PS. The 493 nm<sup>-1</sup> stretching mode vibration of ZnO was observed for ZnO/PS nanocomposite. The PL peak intensity increases due to vacuum annealing treatment.

**Key words:** Porous silicon, ZnO/PS, XRD, SEM, PL, vacuum annealing.

### **Introduction**

In recent years, Silicon based nanocomposites have emerged as a very strong field of research due to their potential applications. The combination of ZnO film and porous silicon substrate would pave the way for integration of ZnO with Si based optoelectronic devices. Porous silicon (PS) is one of the most important Si-based luminescence materials in the field of research. The quantum-sponge model for porous silicon and the geometrical irregularity play an important role in the optical properties of porous silicon [1, 2]. The porous silicon (PS) structure, with a large surface area matrix, is fabricated through electrochemical etching of single-crystal Si wafer in HF based solution [3]. Silicon with various pore sizes is being used in diverse applications such as optical components, gas sensors and micro electro chemical system (MEMS) [4]. The high surface to volume ratio of PS makes it, a possible host material for the precipitation of metals for various applications [1,5].

During the last few years, Zinc oxide emerged as an important oxide material. Zinc oxide is a wide band gap semiconductor with a direct bandgap of 3.3eV at room temperature and exciton binding energy of 60meV [6-8]. ZnO has also gained much interest due to its advantages like good electrical, optical

and piezoelectric behaviors, stability in hydrogen plasma atmosphere and low cost over other oxide thin films such as  $\text{In}_2\text{O}_3$ ,  $\text{SnO}_2$  etc [7]. ZnO is a multifunctional semiconductor material that can be used in many applications such as antireflection coatings, window material for displays and sensors [9]. Therefore, Zinc oxide modified porous silicon (ZnO/PS) composite structures have attracted great interest due to its wide range of applications [1, 10-13].

Different methods have been proposed to deposit ZnO thinfilms on PS layers, such as chemical vapor deposition, a sol-gel process, direct current sputtering and Radio Frequency (RF) sputtering.

In this paper, PS substrates were prepared by electrochemical anodization method for various current densities with constant etching time. The sol-gel spin coating method has been employed to coat ZnO thin film on PS. The structural and optical properties of both PS and ZnO/PS composite were studied in detail.

## Experimental Procedure

### Preparation of porous silicon substrate

PS samples were prepared by electrochemical etching of boron doped p-type (100) oriented Si wafer ( $\rho=0-100\Omega\text{cm}$ ) in a 1:1(48%HF: 99% $\text{C}_2\text{H}_5\text{OH}$ ) solution for 10 minute with different current densities of  $10\text{mA}/\text{cm}^2$ ,  $30\text{mA}/\text{cm}^2$ ,  $50\text{mA}/\text{cm}^2$ ,  $70\text{mA}/\text{cm}^2$  and  $100\text{mA}/\text{cm}^2$  in a Teflon single tank cell. The suitable porous silicon substrate was optimized by studying its structural and optical properties.

### ZnO thin film

The ZnO thin films were coated by sol-gel spin coating method on to the glass substrates for various Zinc concentrations and spin rate to get the optimum experimental condition for obtaining best ZnO thin film. The structural and optical properties of sol-gel spin coated ZnO thin films coated for various Zn concentrations and spin rate have been investigated. It was observed that the grain size of crystallites increases with increase in Zn concentration in the precursor solution. The size of the ZnO grains is lesser for the films prepared 0.3 M Zinc concentration. But as the spin rate of the samples is increased, the grain size value decreases. The optical band gap of the films estimated by UV spectral study increases with decrease in Zn concentration and increase spin rate of the samples. The PL emissions from the films are observed at the wavelength of  $\sim 485\text{nm}$  at room temperature. As a result it can be concluded that the 0.3 M Zinc acetate and 4000 rpm spin rate sample has lesser grain size (24 nm) and higher optical band gap energy (3.26 eV). The structural defect (oxygen vacancies) is also minimum in this sample as per observed PL intensity [14].

### ZnO/PS composite preparation

In order to study ZnO/PS nanocomposite, the ZnO thin film was coated by sol-gel spin coating method at 4000rpm spin rate on optimized PS substrate. To prepare the sol solution, Zinc acetate dihydrate and mono ethanolamine (MEA) were added to 2-methoxy ethanol and the solution was stirred at  $60^\circ\text{C}$  for 2 h to yield a clear and homogeneous solution. The sol-gel coating was made one day after the precursor was prepared. The concentration of Zinc acetate was 0.3M, keeping molar ratio of MEA to Zinc acetate at 1.0. The first sample was prepared by dropping the 0.3M coating solution onto the PS, which was rotated at 4000 rpm for 30 s by using spin coater. The obtained film was dried at  $300^\circ\text{C}$  for 15 minute. The procedure from coating to drying was repeated for six times and then annealed in air at  $550^\circ\text{C}$  for 1 h. To investigate the effect of vacuum annealing on structural and optical properties of ZnO/PS composite, the composite was further vacuum annealed at  $4 \times 10^{-5}$  mbar.

The samples were then characterized by using X'PERT-PRO X-ray diffractometer using the  $\text{CuK}\alpha 1$  radiation ( $\lambda=1.54059\text{\AA}$ ) in The range of  $2\theta$  between  $20^\circ$  and  $80^\circ$ .

The surface morphology of the samples was observed with Shimadzu S-3000N Scanning Electron Microscope and compositional analysis was done by using energy dispersive X-ray spectroscope (EDS). The PL measurements were carried out at room temperature by PerkinElmer LS55 Spectrofluorometer with a He-Cd laser as the excitation source. To obtain the information about chemical bonding, FTIR measurements were performed over range  $400\text{ cm}^{-1}$  to  $4000\text{ cm}^{-1}$  using Shimadzu 8400S Infrared spectrometer.

## Results and Discussion

### Structural properties of PS

#### XRD analysis

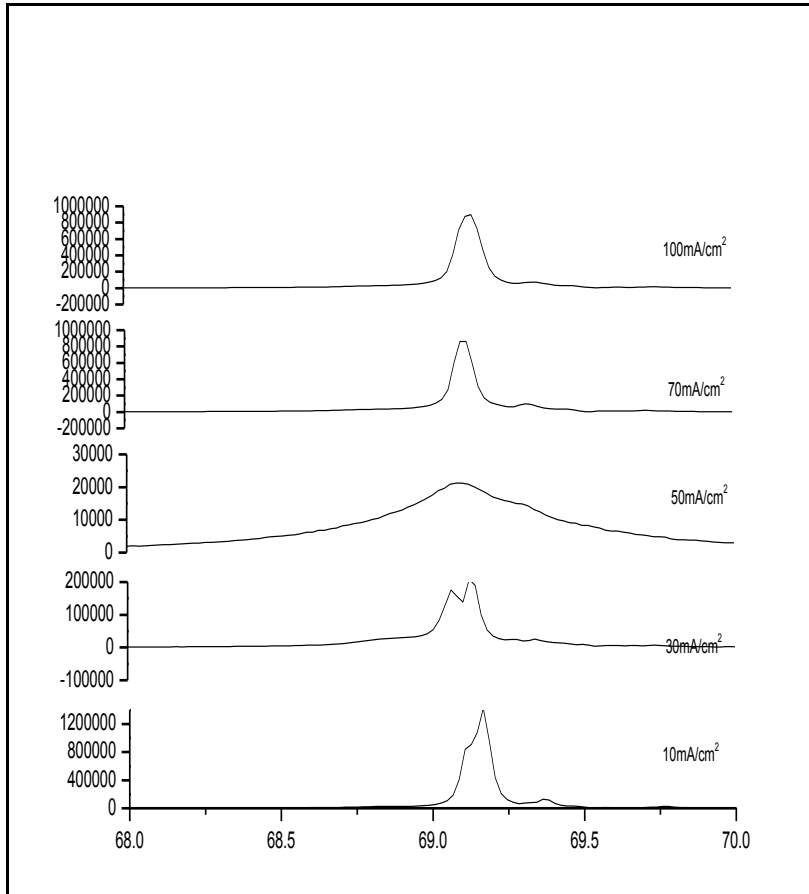


**Figure1: X-ray diffraction pattern of porous silicon for various current densities**

The XRD pattern of porous silicon with different current densities of 10 mA/cm<sup>2</sup>, 30 mA/cm<sup>2</sup>, 50 mA/cm<sup>2</sup>, 70 mA/cm<sup>2</sup> and 100 mA/cm<sup>2</sup> are shown in Figure 1. All the samples show a dominant peak at  $2\theta=69.12^\circ$ . The peak is due to the crystalline Si substrate corresponding to the reflections from (400) set of planes (JCPDS File No.89-2955) [15]. The sample prepared at the current density of 30 mA/cm<sup>2</sup> shows a peak (P1) at  $2\theta=69.1260^\circ$  along with a peak of lower intensity (P2) at  $2\theta=69.0667^\circ$ . The peak P1 is due to the crystalline Si substrate corresponding to the reflections from the (400) set of planes. The shorter peak arises from the porous layer [16]. The 50 mA/cm<sup>2</sup> sample shows a broad peak indicating small and uniform grains all over the surface. Increasing the current density above 50 mA/cm<sup>2</sup> the upper layer could have been etched away and the grain size value corresponds to grains of the next layer [17]. The grain size  $D$  of crystallites was calculated from the Scherer's formula,

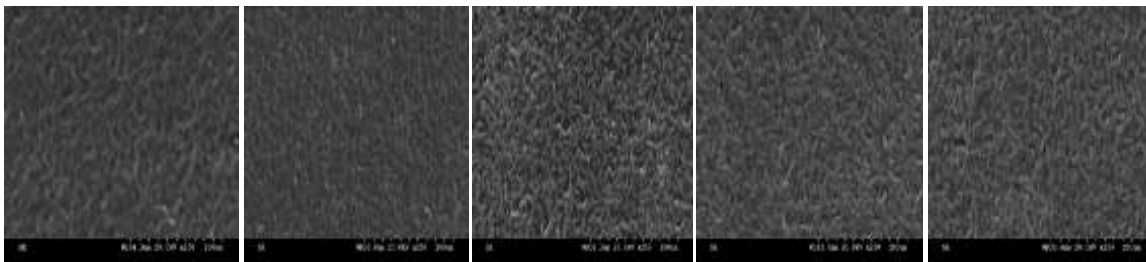
$$D = \frac{0.9\lambda}{\beta \cos\theta}$$

where  $D$  is the grain size of crystallite, ( $\lambda=1.54059\text{\AA}$ ) is the wavelength of X-ray used,  $\beta$  is the broadening of diffraction line measured at half its maximum intensity in radians and  $\theta$  is the angle of diffraction. The grain size value of silicon crystallites calculated for the samples are shown in Table 1. The grain size calculated for the sample prepared at 50 mA/cm<sup>2</sup> current density is 17 nm and this indicates that the surface has widened pores.

**Table 1: Grain size and FWHM values for the PS samples**

Current Density(mA/cm <sup>2</sup> )	2θ(Degree)	Peak Height(a.u)	FWHM	Grain size D(nm)
10	69.1654	1428011	0.0986	98
30	69.1260	208495	0.1183	82
	69.0668	175216	0.1380	70
50	69.1062	21285	0.5719	17
70	69.1260	861611	0.0789	122
100	69.1457	896903	0.1183	82

### Surface morphology analysis



(a) (b) (c) (d) (e)

**Figure 2: SEM images of PS prepared for various current densities (a) 10mA/cm<sup>2</sup> (b) 30mA/cm<sup>2</sup> (c) 50mA/cm<sup>2</sup> (d) 70mA/cm<sup>2</sup> (e) 100mA/cm<sup>2</sup>**

SEM images (Figure 2a-e) show the top view of the samples prepared for various current densities at 10 minute. The porosity (P) can be defined as a function of geometrical parameters written as [18],

$$P = \left( \frac{\pi}{2} * 1.732 \right) \left( \frac{1}{1 + \frac{m}{d}} \right)^2$$

where d is the average pore size and m is the distance between pores. The calculated porosity value for the samples prepared for 10,30,50,70 and 100mA/cm<sup>2</sup> was found to be 30,45,79,58 and 61%. The porosity value 79% for the sample prepared at 50mA/cm<sup>2</sup> current density is the highest obtained among all the samples. This porous silicon sample was considered to coat ZnO thin film.

### Photoluminescence studies

The PS samples exhibit a PL emission peak at 606nm (Figure 3). SEM study of the PS sample prepared at current density 50mA/cm<sup>2</sup> shows that the porosity is maximum and this is supported by maximum PL intensity.

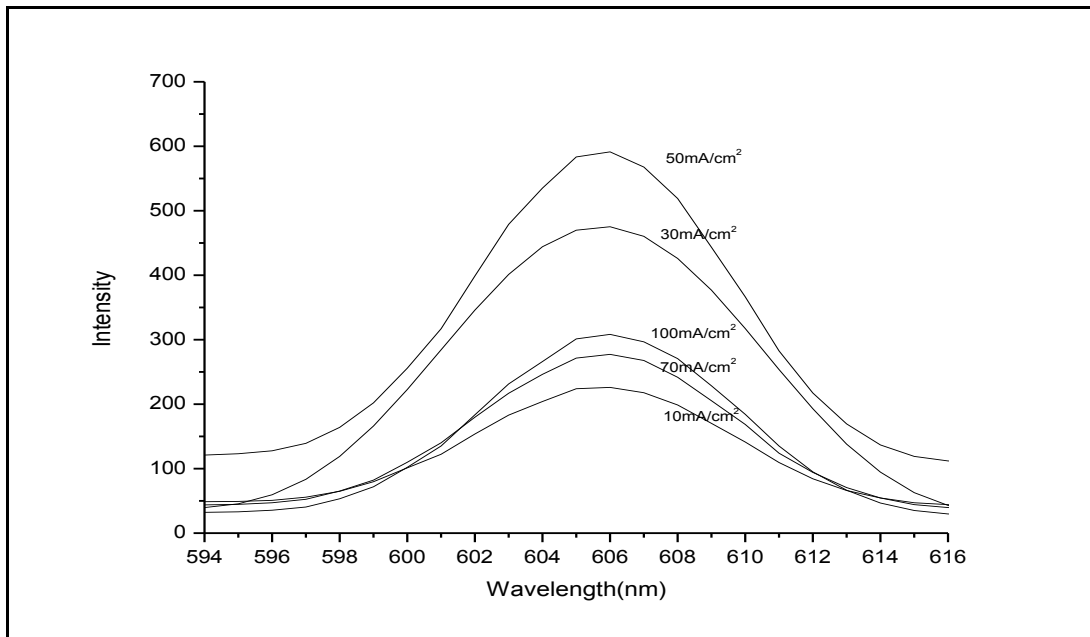


**Figure 3: PL spectrum of PS for various current densities**

### Structural properties of ZnO/PS

#### XRD analysis

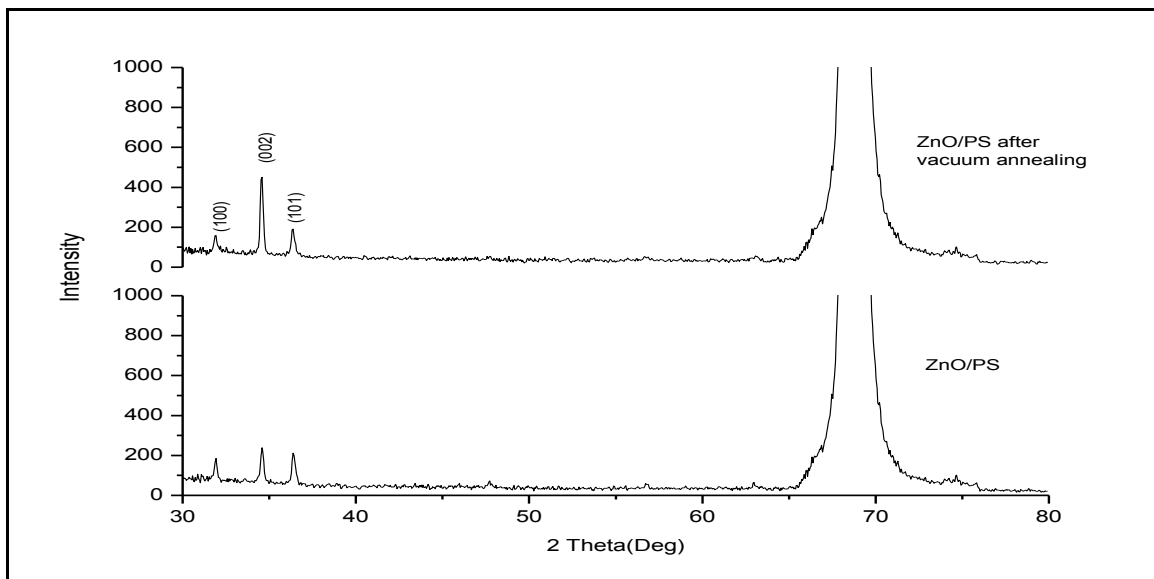


**Figure 4: X-ray diffraction pattern of ZnO/PS composite**

Figure 4 shows the X-ray diffraction pattern of the ZnO thin film on Porous silicon (ZnO/PS) and vacuum annealed ZnO/PS respectively. The diffraction peaks of (002), (101) and (200) orientations are correspond to ZnO thin films and shows the polycrystalline nature of ZnO on porous silicon substrate[2]. From Figure 4 the predominated c-axis (002) peak confirms the hexagonal wurtzite structure of ZnO(JCPDS,36-1451) and shows that the ZnO thin film formed on PS substrate is highly c-axis oriented. The broadening around 68.95° is attributed to the silicon nanocrystallites[15]. The grain size of ZnO crystallites on PS and vacuum annealed PS were calculated for (002) peak and the values are 49nm and 61nm respectively. This shows that the increased interaction at the interface of PS and ZnO. Current density plays an important role in the formation of porous silicon; at wider pores the ZnO nanoparticles can accommodate and the crystalline quality of the ZnO thin film increased with the porosity of the porous silicon substrate. After vacuum annealing,

it can be seen that the (002) peak becomes harper and its full-width half maximum (FWHM) value decreased from 0.1768 to 0.1412, this indicates that the crystallinity of ZnO thin films is enhanced on vacuum annealing. From the XRD results, it can be observed that the porous silicon can work as a good substrate for ZnO growth due to its special surface morphology[19].

The lattice constants  $a$  and  $c$  were calculated respectively from (100) and (002) peaks, by using the well-known formula of analytical method is given by

$$\frac{1}{d^2} = \frac{4(h^2+hk+k^2)}{3a^2} + \frac{l^2}{c^2}$$
 whereh,k,l represent the lattice planes and d is the interplanar distance. The Zn-O bond length L was calculated by,

$$L = \sqrt{\left(\frac{a^2}{3c^2} + \left(\frac{1}{2} - u\right)^2 c^2\right)}$$

where the parameter  $u$  for Wurtzite structure related to  $a$  and  $c$ , is given by  $u = \frac{a^2}{3c^2} + 0.25$

The FWHM, grain size, lattice constants and Zn-O bond length values for (002) peak are shown in Table 2. Strain and stress values of the films were calculated by using the values of the lattice spacing obtained from XRD results.

The corresponding stress values were calculated using the equation

$$\sigma = -233 \times 10^9 \varepsilon^{hkl}$$

where  $\varepsilon^{hkl} = \frac{(d^{hkl} - d_0^{hkl})}{d_0^{hkl}}$  is the elastic strain of the (hkl) planes,  $d_0^{hkl}$  is the strain free lattice spacing of the

(hkl) lattice plane and  $d^{hkl}$  is the lattice spacing of the (hkl) plane of the film[20]. The stress and strain values of ZnO thin films are also shown in Table3. The obtained stress values are positive for ZnO thin films coated on PS which confirms the biaxial stress is tensile and the strain measured for this film is compressive. After vacuum annealing treatment  $2\theta$  value of PS reduces to  $34.538^\circ$  from  $34.561^\circ$  and it implies the decrease in residual stress. This may decrease the formation of dislocation and cracks in ZnO thin films [19]. This also confirmed by decrease in ZnO bondlength after vacuum annealing [21].

**Table 2. The FWHM, grain size, lattice constants and ZnO bond lengths of ZnO thin films calculated for (002) peak.**

ZnO films on	2 $\theta$ (deg)	FWHM (deg)	Grain size (nm)	a (nm)	c (nm)	Bond length( $\text{\AA}$ )
Porous silicon	34.561	0.1768	49	0.3238	0.5186	1.9716
Porous silicon (vacuum annealed)	34.538	0.1412	61	0.3239	0.5188	1.9710

**Table 3: Stress and strain values of ZnO thin film**

ZnO films on	Strain	Stress (* $10^9$ pa)
Porous silicon	-0.003956	0.9217
Porous silicon (vacuum annealed)	-0.003572	0.8322

### Surface morphology analysis

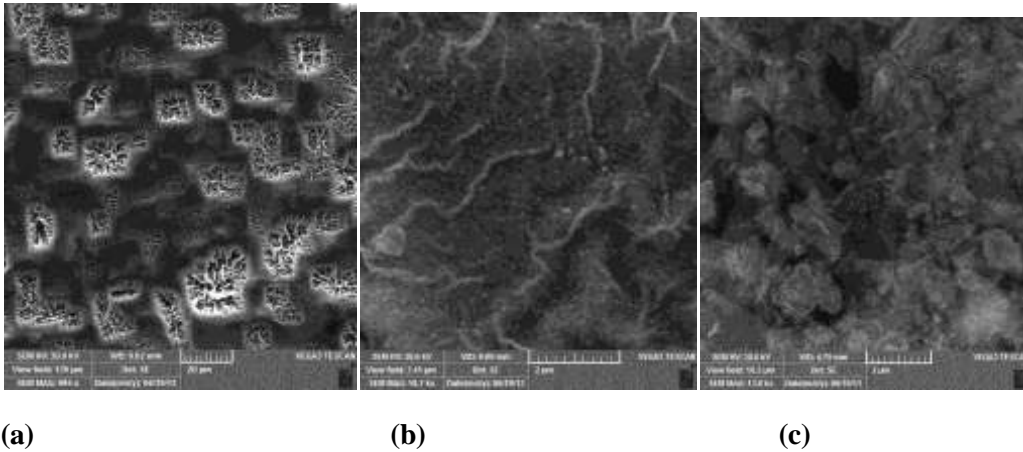


**Figure 5: SEM images of a) ZnO on PS and magnified images b) before and c) after vacuum annealing**

The ZnO crystallites deposited on porous silicon substrate can be observed from the magnified SEM images before and after vacuum annealing (Figure 5 b,c). The SEM image reveals that the most of the pores were filled with ZnO nano particles.

An energy dispersive X-ray (EDS) spectrum of ZnO/PS and vacuum annealed ZnO/PS are shown in Figure 6a, b. The peaks associated with Si, Zn and O atoms are seen in this spectrum (the Al related peak in the spectrum is due to the Al back contact). EDS spectrum confirms the presence of Zn and O.

On vacuum annealing, the chemisorptions of large number of oxygen molecules at the grain boundaries on the surface of the films desorbed from the samples. From the Figure 6b (after vacuum annealing) it was observed that the stoichiometry ratio was changed between Zn and O. Vacuum annealing also shows that the strong interaction of ZnO with the PS surface.

### FTIR analysis

Figure 7 presents the FTIR spectra of ZnO/PS composite before and after vacuum annealing. The peaks observed at  $623,860$  and  $910\text{cm}^{-1}$  are due to the Si-H and Si-H<sub>n</sub> structural groups respectively [22,23]. Thus the chemisorptions of Si-H<sub>n</sub> in the PS layer are closely linked to the variation in PL intensity. The absorbance bands at  $870$  and  $974\text{cm}^{-1}$  are caused by Si-O and Si-O-H formation. The band observed between  $1050$  and  $1250\text{cm}^{-1}$  are due to the presence of Si-O-Si bonds [24,25].

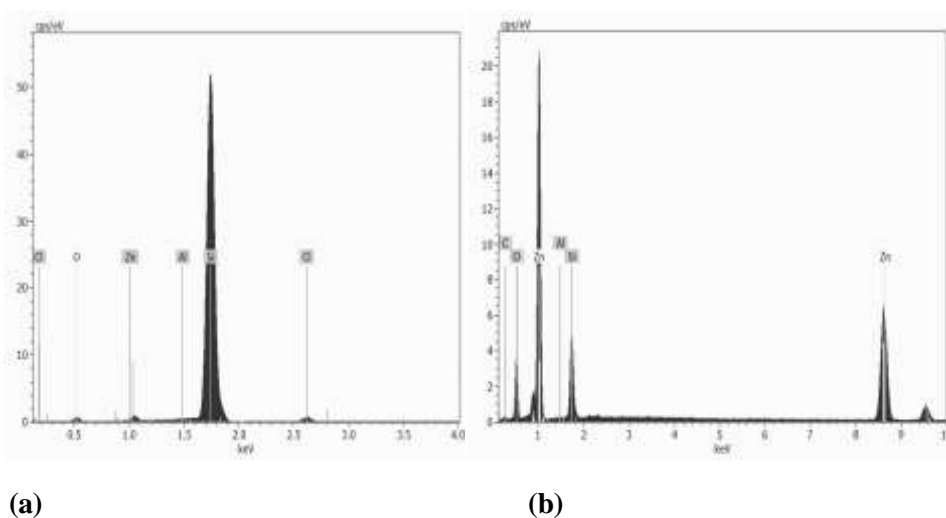


**Figure 6: EDS spectrum of ZnO on PS (a) before (b) after vacuum annealing**

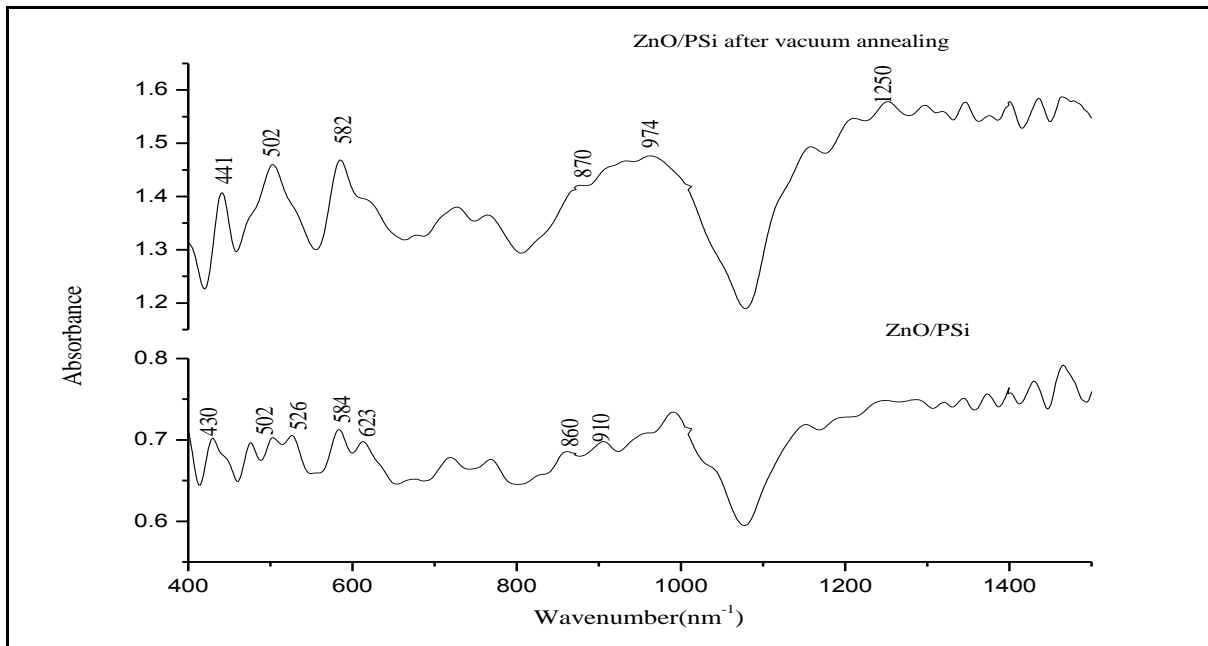


**Figure 7: FTIR spectra of ZnO/PS before and after vacuum annealing**

The FTIR spectra of ZnO/PS show a peaks at 441, 502 and 582  $\text{cm}^{-1}$  which belongs to Zn-O stretching [26]. After vacuum annealing the FTIR absorption peak intensity increases in ZnO/PS composite and the intensity of Si-H<sub>n</sub> peaks are found to be decrease in ZnO/PS composite. This may be due to oxygen passivation after ZnO coating on PS surface.

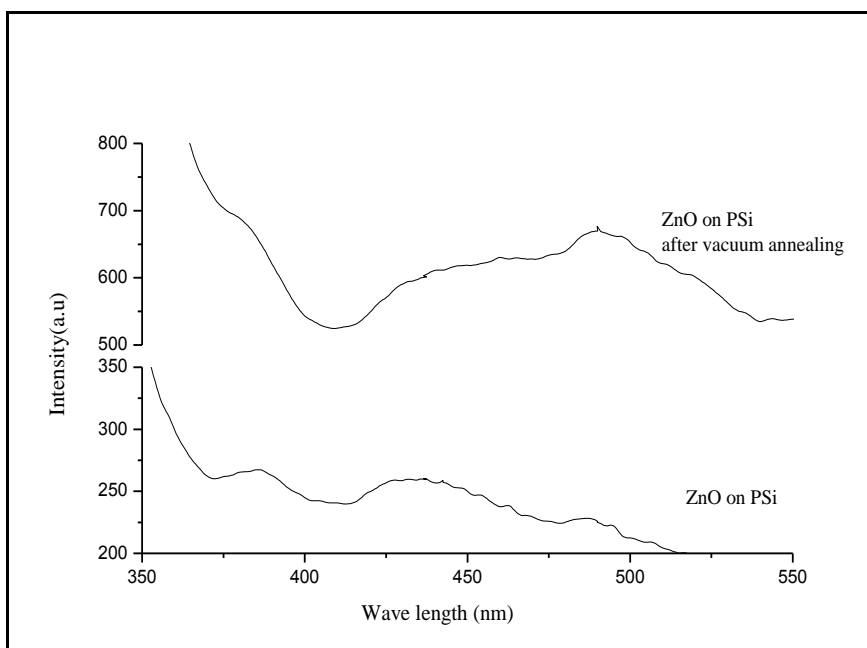


**Figure 8: PL spectrum of ZnO/PS nano composite before and after vacuum annealing**

Figure 8 shows the PL emission spectra of ZnO/PS nanocomposite before and after vacuum annealing treatment. The UV emission peak at 386 nm and violet emission peak at 430 nm were observed in the ZnO/PS composite [27]. The first one is due to the free exciton emission and the other one is correspond to the Zn or Oxygen vacancies. After vacuum annealing, the both the peaks are found to be disappeared and the broad green emission peak at 485 nm was observed and that is due to the ZnO deep level emission [28]. The intensity of emission peak increases for vacuum annealed ZnO/PS and this may be the reason of increase in grain size of ZnO at vacuum annealing and this is confirmed by XRD data. There is no PL peak for porous silicon was seen.

This shows that ZnO deposited on PS could change the surface structure and reduces the Si-H<sub>n</sub> species. The Si-H<sub>n</sub> bonds play an important role in the luminescence properties of PS [10]. Formation of Si-O bonds would break the Si-H bonds after ZnO deposition on the PS surface [2].

## Conclusion

The structural and optical properties of PS samples prepared for various current densities have been investigated. SEM images reveal the formation of porous surface and uniform distribution of pores in the porous layers. At 50mA/cm<sup>2</sup> the value of porosity is maximum and pores are widened. Visible PL was observed at 606 nm and its intensity is maximum for the sample prepared at 50mA/cm<sup>2</sup>. The 0.3M Zinc acetate was coated on PS prepared at 50mA/cm<sup>2</sup> by sol-gel process method. X-ray spectra confirm the presence of ZnO on PS. After vacuum annealing the grain size of ZnO on PS increases from 49 to 61 nm. The 512cm<sup>-1</sup> stretching mode vibration was observed for ZnO on PS. The two PL peaks were obtained for ZnO on ZnO/PS nanocomposite at 380 nm and 485 nm respectively. The first one is due to free exciton emission and the second one is due to oxygen vacancies in ZnO. From the results it can be observed that PS can work as a good substrate for ZnO growth. Therefore, the ZnO/PS composite structure can be used as a solid source for various potential applications.

## References

1. LiuYL, LiuYC, Yang H, Wang WB, MaJG, Zhang JY, LuYM, ShenDZ and FanXW, The optical properties of ZnO films grown on porous Si templates. *J. Phys. D: Appl. Phys.*, (2003)36;2705-2708.
2. Singh RG, Singh F, Agarwal V and Mehra RM, Photoluminescence studies of ZnO/Porous silicon nanocomposites, *J. Phys. D: Appl. Phys.*, (2007)40;3090-3093
3. Wang J, Guo DJ, Xia B, Chao J, Xiao SJ, Preparation of organic monolayers with azide on porous silicon via Si-N bonds, *Colloids and Surfaces A*: (2007) 305;66-75
4. Abramof PG, Beloto AF, Ueta AY, Ferreira NG, X-ray investigation of nanostructured stain-etched porous silicon, *Appl. Phys.*, (2006)99;024304
5. Jiang T, Zhou X, Zhang J, Jianzhong, Li X, Li T, Study of humidity properties of Zinc Oxide modified Porous Silicon, *IEEE Sensors Exco*, Daegu, Korea (2006)22-25
6. Caglar M, Ilican S, Caglar Y, Influence of Substrate temperature on structural and electrical properties of ZnO films, *Trakya. Univ. J. Sci.* (2006)7;153.
7. Lee JH, Ko KH, Park BO, Electrical and optical properties of ZnO transparent conducting films by the sol-gel method, *J. Cryst. Growth.* (2003) 247;119.
8. Kuo SY, Chen W, Lai F, Cheng CP, Kuo HC, Wang SC, Hsieh WF, Effects of doping concentration and annealing temperature on properties of highly oriented Al-doped ZnO films, *J. Cryst. Growth.* (2006)287;78-84
9. Sun E, Su FH, Shih YT, Tsai HL, Chen CH, Wu MK, Yang JR, Chen MJ, An efficient Si light emitting diode based on n-ZnO/SiO<sub>2</sub>-Si nanocrystals-SiO<sub>2</sub>/p-Si heterostructure, *Nano Technology.* (2009) 20;445202
10. Hanan A, Abdulla T, Suhail M, Naji AN, Al-Zaidi OG, Ghaida S, Muhammed, Naum FA, Fabrication and characteristics of fast Photo response ZnO/Porous Silicon UV Photoconductive Detector, *Advances in Materials Physics and Chemistry.* (2011)1;70-77
11. Li X, Zhang B, Zhu H, Dong X, Xia X, Cui Y, Ma Y, Du G, Study on the luminescence properties of n-ZnO/p-Si hetero-junction diode grown by MOCVD, *J. Phys. D: Appl. Phys.* (2008)41;035101
12. Cai H, Shen H, Yin Y, Lu L, Shen J, Tang Z, The effects of porous silicon on the crystalline properties of ZnO thin films, *Journal of Physics and Chemistry of Solids.* (2009)70;967-971
13. Hsu HC, Cheng CS, Chang CC, Yang S, Chang CS, Hsieh WF, Orientation-enhanced growth and optical properties of ZnO nanowires grown on porous silicon substrates, *Nano Technology.* (2005)16;297-301
14. Lakshmipriya V, Natarajan B, Jeyakumaran N, Prithvikumaran N, Structural and Optical properties of ZnO thin films prepared by spin coating method — influence of concentration and spin rate, *Surf. Rev. Lett.* (2012)19;1250018
15. JCPDS File No. 89-2955 (International Centre for Diffraction Data) Newton Square, PA, U.S.A.
16. Tischler, *Phys. Today.* (1996)50;24

17. Vidhya VS, PadmavathyP, Murali KR, Sanjeevi raja C, Manisankar P, Jayachandran M, Development of porous silicon matrix and characteristics of porous silicon/tin oxide structures. *J. Non-crystalline solids.*(2011)357;1522-1526.
18. Cai H, Shen H, Lu L, Huang H, Tang Z, Yin Y, Shen J, Properties of the ZnO/PS nanocomposites obtained by sol-gel method, *Optoelectronics and advanced materials.*(2010)4;650-653
19. Welzel U, Ligot J, Lamparter P, Vermeulen AC, Mittemeijer EJ, Stress analysis of polycrystalline thin films and surface regions by X-ray diffraction, *J. Appl. Cryst.*(2005)38;1-29
20. KimMS, YimKG, Leem JY, Kim S, Nam G, Lee DY, Kim JS, Sukim J, Thickness Dependence of Properties of ZnO Thin films on Porous Silicon Grown by Plasma-Assisted molecular beam Epitaxy, *Journal of the Korean Physical Society*,(2011)59;2354-2361
21. Natarajan B, Ramakrishnan V, Vasu V, Ramamurthy S, Structural and Photoluminescence Properties Of Porous Silicon: Effect of Surface Passivation, *Surface review letters.*(2005)12;645-649
22. Hilliard J, Andsager D, Abu Hassan L, Nayfeh HM, NayfehMH, Infrared Spectroscopy and secondary ion mass spectrometry of luminescent, nonluminescent and metal quenched porous silicon, *J. Appl. Phys.*(1994)76;
23. Aprelev AM, Lisachenko AA, Laiho R, Pavlov A, Pavlova Y, UV ( $h\nu=8.43$  eV) photoelectron spectroscopy of porous silicon near Fermi level, *Thin solid films.* (1997)297;142-144
24. HoryMA, HerinoR, LigeonM, MullerF, Gaspard F, MihalcescuI, VialJC, Fourier transform IR monitoring of porous silicon passivation during post-treatments such as anodic oxidation and contact with organic solvents, *Thin solid films.*(1995)255;200-203
25. DubinVM, Ozanam F, Chazalveil JN, In situ luminescence and IR study of porous silicon during and after anodic oxidation, *Thin solid films.*(1995)255;87-91
26. Swanboon S, Structural and Optical Properties of Nanocrystalline ZnO Powder from Sol-Gel Method, *Science Asia.* (2008)34;031-034
27. Bo LX, Lie SH, Hui Z, BinLB Optical properties of nanosized ZnO films prepared by Sol-gel process, *Trans. Nonferrous Met. Soc.* (2007)17;s814
28. Kang HS, Kang JS, Kim JW, Lee SY, Annealing effect on the property of ultraviolet and green emissions of ZnO thin films, *J. Appl Phys.*(2004)95;1246.

\*\*\*\*\*